ISSN: 2692-5397
DOI: 10.33552/MCMS.2024.05.000641
Modern Concepts in Material Science
Iris Publishers
Research article

Fast decoration of titanium nanoparticles with noble metals for enhanced visible-light photocatalytic activity in environmental remediation and hydrogen generation

Ceren Uzun[1], Naden Erabe[2], Murat Kaya[1]*

[1]*Department of Chemical Engineering, Atılım University, 06830 Ankara, Turkey*

[2]*Graduate School of Natural and Applied Science, Atılım University, TR-06830 Ankara, Turkey*

***Corresponding author:** Murat Kaya, Department of Chemical Engineering, Atılım University, 06830 Ankara, Turkey

Received Date: September 02, 2024

Published Date: September 17, 2024

Graphical Abstract

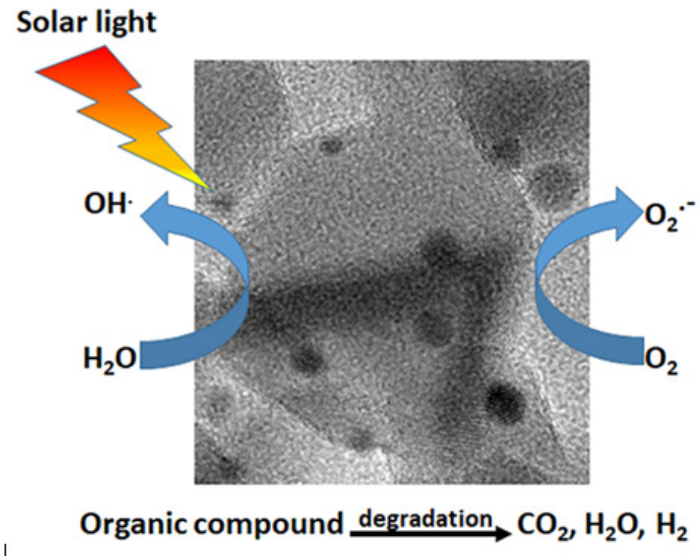

Highlights

- Fast and facile decoration of TiO_2 nanoparticles with ultra-small bimetallic AgAuNPs is achieved (1h in total).
- High catalytic activities were observed with the addition of noble metals under both UV and visible light illuminations.
- Besides the total degradation of methylene blue (64 mg L-1) in a short time, hydrogen generation from the water-ethanol mixture (10% ethanol) was observed without needing H_2O_2.

Abstract

Highly efficient photocatalyst working under visible light was prepared by the decoration of plasmonic silver, gold and bimetallic silver-gold nanoparticles on the TiO_2 nanoparticles by using fast, simple and green method. Decoration of plasmonic nanoparticles was achieved easily in 1 h with the addition of metal ions onto the TiO_2 nanoparticles in aqueous solution followed by $NaBH_4$ reduction. Characterization of catalysts was performed by TEM, EDX coupled to TEM, BET, XPS, and ICP-OES. The photocatalytic efficiency of the plasmonic nanoparticles added TiO_2 nanoparticles in the degradation of methylene blue in aqueous solution were investigated under both UV and solar light exposure, respectively. Degradation of MB was followed with UV-Vis spectrometry and confirmed with LC-MS. The photocatalytic activity of the prepared nanoparticles also tested in the hydrogen evolution from the water-ethanol mixture under UV light irradiation. The amount of hydrogen gas obtained from the photocatalytic reaction was determined by GC-TCD.

Keywords: Semiconductor photocatalyst, Noble-metal doping, Environmental remediation, Hydrogen production

Introduction

For the environment and ecosystem, the elimination of pollutants from industrial waste is crucial. As a synthetic dye, azo dyes have aromatic structure making them extremely stable, so that they are known as nonbiodegradable carcinogens. The release of such dyes even in small quantities causes major adverse effects to humans via the food chain due to contaminated water resources [1,2].

One of the most effective ways for removing organic based pollutants from water and obtaining hydrogen from volatile organic compounds founded in wastewaters is known as the photocatalytic process. The effectiveness and cheapness of the method have been proven for the degradation of pollutants and the production of hydrogen under UV and visible light [3].

In this process, it is very important to produce cheap and efficient catalysts with an energy level suitable for working with solar radiation [4,5]. As known, the efficiency of the photocatalytic process depends on the separation of the photogenerated electrons and holes and the reduction of the charge recombination. Therefore, extremely stable, having the capability to work in a wide variety of light sources such as UV, visible, near-infrared (NIR) as well as natural solar light and having low recombination rates are crucial factors to produce photocatalysts. In this direction, numerous studies are carried out to increase charge separation efficiency and interfacial contact [6].

Rapid industrialization and consequently the excessive use of non-renewable energy sources have caused not only the rapid depletion of energy resources but also the toxic wastes accumulated in the environment reaching dangerous levels. Therefore, renewable energy sources produced by environmentally sensitive methods are needed in order to reduce the harm to the environment while meeting the energy demand [7,8]. As clean energies, hydrogen energy is considered as an alternative to fossil fuels due to having high gravimetric energy density and effective methods that make its use widespread are being investigated [9].

Heterogeneous photocatalysis can be identified as speeding up the photochemical process in the presence of a catalyst. Even though history and research related to heterogeneous photocatalysis trace back to many decades, after the reports published by Fujishima and Honda in 1972, the field of heterogeneous photocatalysis has expanded extensively. The discovery named ''Honda-Fujishima Effect'' describes the photocatalytic phenomenon related to electrolysis of water in the presence of TiO_2 [10]. Since this time, semiconducting catalyst materials have gained great attention on the use of such materials for the environmental and energy applications such as degradation of pollutants in air and water, and solar energy conversion and fuel production through redox processes.

Among several semiconductors, particularly titanium dioxide (TiO_2) is close to being an ideal photocatalyst due to its strong oxidation properties, high photochemical and biological stability, non-toxicity, and low cost [11,12]. However, the polymorphs of TiO_2 named anatase, rutile, and brookite have large bandgap values with 3.2, 3.02 and 2.96 eV respectively [13]. Accordingly, the large bandgap results in the excitation only by UV light and exhibits charge carrier recombination in nanoseconds. For these reasons, in order to increase the interfacial charge-transfer process and on account of photocatalytic activity of TiO_2 under Vis radiation, the modification of the catalyst surface with noble metal nanoparticles (NP's) can be applied.

Among the noble-metal based nanoparticles, Ag and Au NPs are of interest due to their strong surface plasmon resonance (SPR) absorption in the visible part of the spectrum which is directly related to their size and shape [14]. Besides the effect on SPR, the size of the noble metal nanoparticles has direct role in photocatalytic efficiency [15-17] Decoration of the surface of the TiO_2 nanoparticle with small-sized noble metal nanoparticles resulted in a highly efficient visible-light-driven photocatalyst by shifting Fermi level energy of TiO_2 nanoparticles which allows the rapid electron transfer and thus improved charge separation [18-22].

There are many studies recently published related to the usage of noble-metal decorated TiO2 nanoparticles as photocatalyst in environmental and energy applications [15-22]. But, the preparation of size-controlled metal nanoparticles like silver and gold or bimetallic form of them (ranges from 2 to 5 nm) on the surface of TiO2 and providing narrow size distribution is still challenging. Conventional techniques such as photoreduction, sonochemical, radiolysis, microemulsion, deposition-precipitation, hydrothermal and chemical reduction methods generally generate aggregated photocatalysts in bigger sizes with low crystallinity. Besides, these techniques need several and complicated steps for production [23-28].

In the light of the photocatalytic potential of TiO_2 and optical properties and SPR behavior of Au, Ag noble metal nanoparticles, ultra-small size AuAg nanoparticles decorated TiO_2 nanoparticles work under UV and solar light irradiations were prepared by using a green and fast method. The photocatalytic activity of the prepared catalyst was studied toward the degradations of an azo dye, methylene blue, in water and hydrogen production from the water-ethanol mixture. Comparison of the catalytic performance of AuAg nanoparticles decorated TiO_2 (TiO_2-AgAuNPs) with bare TiO_2, TiO_2-AgNPs, and TiO_2-AuNPs, was also performed. Degradation of methylene blue and hydrogen generation was demonstrated with the determination of degradation products and hydrogen gas by using LC-MS and GC-TCD, respectively.

Experimental

Materials

A commercial form of TiO_2 (Degussa, P25, the surface area of 50 $m2g^{-1}$) was used as support for the preparation of photocatalysts. Sodium borohydride ($NaBH_4$), ethanol, silver nitrate ($AgNO_3$) and gold(III) chloride trihydrate ($HAuCl_4 \cdot 3H_2O$) and methylene blue (MB) dye for photocatalytic degradation studies were obtained from Sigma Aldrich. All chemicals were analytical grade and used as received. Deionized water (Milli Q with 18.6 MΩ) was utilized in all reactions and preparation processes.

Preparation of Metal Nanoparticles Loaded TiO_2

Preparation of photocatalyst (TiO_2-M) was obtained by the decoration of the noble metal nanoparticles M (M= Ag, Au, and AgAuNPs, respectively) on TiO_2 nanoparticles. For this, initially, 100 mg TiO_2 nanoparticles were dispersed into 10 mL water containing the needed amount of metal precursor (the total mass percentage was 2.0 %(w/w) with respect to support) and kept in the ultrasonic bath for 5min. After that, the mixture was further stirred with magnetic stirrer vigorously for 25 min. At the end of the mixing period, particles were collected and washed. The supernatant and washing portions were kept for finding the exact amount of metal ions (Ag(I), Au(III)) loaded onto the TiO_2 support with ICP-OES. After the washing step, particles were dispersed in 10 mL water for the reduction of ions added onto the surface by using $NaBH_4$. After a short reduction period samples were centrifuged, washed and used directly in the photocatalytic process. The same procedure was applied for both mono and bimetallic nanoparticles added photocatalyst. In the case of the catalyst containing bimetallic nanoparticles (TiO_2-AgAu), the three different ratios of Ag: Au (3:1, 1:1 and 1:3) were performed and continued with the one which shows the highest activity.

Catalytic Activity Measurements

The photocatalytic activities of TiO_2-M nanoparticles evaluated using methylene blue (MB) as a wastewater pollutant model compound under UV and solar light irradiation by following the decrease in the absorbance value of the aqueous solution of MB dye located at 660 nm. The photocatalytic reactions were performed with UV (Hg-lamp, 150 W) and solar (Xe-Arc lamp, 300 W) lights. In order to prevent the direct interaction of lamps with a reaction medium and cool the lamp by using a circulator, a glass jacket made of quartz was used for UV light exposure. The mixture was initially stirred with a magnetic stirrer for 10 min under dark to provide adsorption/desorption equilibrium. After that mixture was irradiated with light and a 2 mL sample was taken every 10 min and decolorization of MB was measured with a UV-Vis spectrophotometer. After getting all data the percent removal of MB which shows the photocatalytic efficiency of the catalyst was calculated from the obtained absorbance values (A) by using the equation given below (Eq. 1)

$$D = (A_0\text{-}A_t)/A_0 \times 100\ \% \qquad (1)$$

(D= percent degradation of dye molecules, A_0=initial absorbance of dye solution, A_t=absorbance of dye solution after a certain at time) For reuse studies, the photocatalyst was isolated, washed and used for the next cycle of catalytic reaction with a fresh MB solution. Products formed at the end of the photo-degradation of MB were analyzed through LC-MS.

The photocatalytic hydrogen evolution ability of the prepared catalysts was tested by using a water-ethanol mixture. In a typical test photocatalyst (20 mg) was suspended in 50 mL of 10 vol% aqueous ethanol before exposing the system. The reactor temperature was maintained at 25ºC with the help of a circulator. The quantification of the hydrogen gas obtained was done by GC–TCD (Agilent 7890B).

Results and Discussion

Morphology of the Prepared Catalysts

TiO_2-M (M: Au, Ag and AgAuNPs) nanoparticles were produced by initially doping of the metal ions onto the surface of TiO2 nanoparticles followed with the chemical reduction in water. After that TEM (JEM-2100F (JEOL) operated at 200 kV) measurements were performed to figure out the particle size and distribution of metal nanoparticles (Ag, Au, and AgAuNPs) decorated onto the TiO_2 nanoparticles. The results are given in Figure 1.

From Figure 1(a), the average size of the individual TiO_2 nanoparticles in the aggregates was measured around 25 nm. TEM images show that the spots over support indicate that small AgNPs (~4-8 nm, Figure 1(b)) and AuNPs (~6-10 nm, Figure 1(c)), and ultra-small AuAgNps (~2-3 nm, Figure 1(d)) distributed uniformly on TiO_2 nanoparticles.

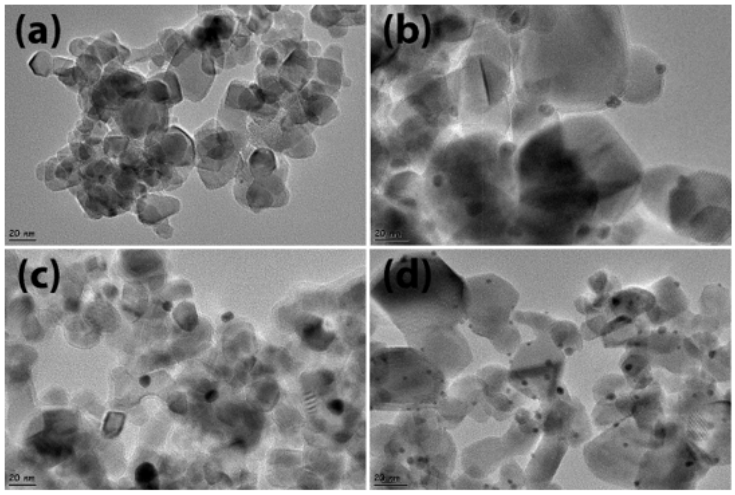

Figure 1: TEM images of bare TiO_2 nanoparticles (a), TiO_2-AgNPs (b), TiO_2-AuNPs (c) and TiO_2-AgAuNPs (d).

TEM image of TiO_2-AgAuNPs (Figure 2-d) exhibits homogeneous particle distribution on the surface. Interestingly, the size of the bimetallic nanoparticles produced on the surface of TiO_2 nanoparticles is smaller compared to the silver and gold nanoparticles added separately. It is known that the structure and morphology of bimetallic nanoparticles strongly depend on the synthetic procedure and miscibility of two metals. Bimetallic nanoparticles exhibit distinct unique properties than that of corresponding pure monometallic counterparts and their physical mixings. Therefore, they show better photocatalytic performance compared to monometallic ones. Generally, bimetallic nanoparticles have smaller crystallite size which can be attributed to a decrease in both enthalpy and Gibbs free energy of bimetallic nanoparticles during synthesis.

The chemical composition of the metal nanoparticles added TiO_2 nanoparticles was investigated with the energy-dispersive X-ray (EDX) spectroscopy coupled to TEM as shown in Figure 2 (a-c). The results show that the TiO_2 nanoparticles (Degussa P25) contain the silver and gold elements which are considered as the indications of the addition of Ag, Au, and AgAuNPs onto the support material. Quantification of the added metal nanoparticles over the support was performed by using ICP-OES (Perkin-Elmer DRC II model). The weight percents of the metal nanoparticles were calculated as 1.15 % (w/w) for AgNPs, % 0.52 (w/w) for AuNPs and and % 0.68 (w/w, Ag) and % 0.45 (w/w, Au) for bimetallic AgAuNPs, respectively.

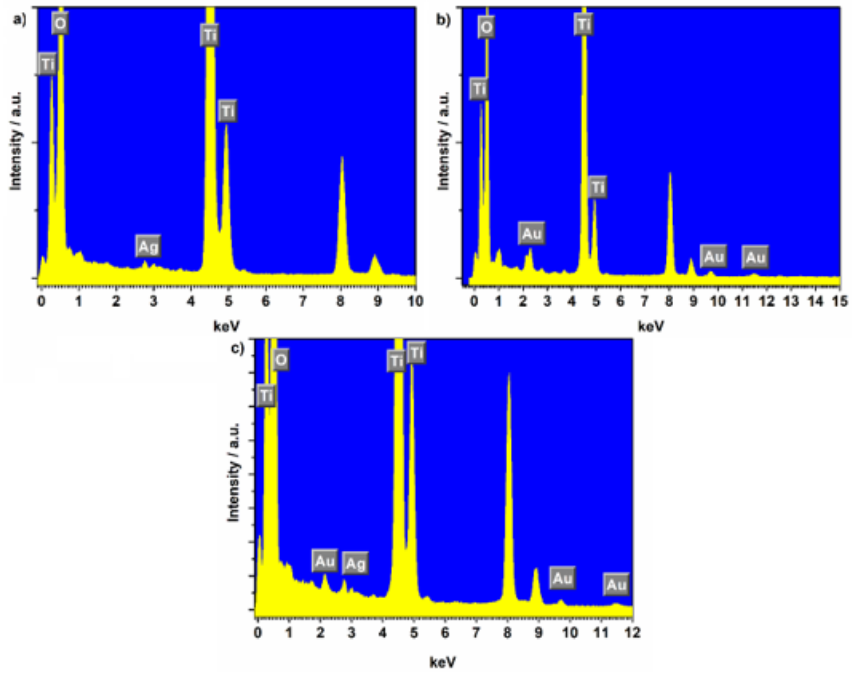

Figure 2: EDX images of TiO_2-AgNPs (a), TiO_2-AuNPs (b) and TiO_2-AgAuNPs (c).

BET Measurements

The specific surface areas of the bare TiO_2 nanoparticles (Degussa P25) and catalysts obtained with the addition of bimetallic Ag and Au nanoparticles onto TiO_2 nanoparticles prepared catalysts were investigated with Brunauer– Emmett–Teller (BET) N_2 adsorption-desorption measurements (BET, Micromeritics ASAP 2020, USA). The surface area of TiO_2 (Degussa P25) was found from BET (Brunauer–Emmett–Teller) plot as 52 m2/g. The surface area of the TiO_2 nanoparticles (Degussa P25) decreased 47.0 m2/g after the addition of noble metal NPs (AgAuNPs, 0.68% Ag, 0.45% Au) which indicates the decoration of TiO_2 nanoparticle surface with bimetallic metal nanoparticles. As known a higher surface area is the indication of better catalytic activity due to more interaction of the target molecule with the surface of the catalyst. But, in this case, the addition of metallic nanoparticles is more effective on photocatalytic activity than the effect of the reduction in surface area due to an increase in the charge transfer ratio between the target molecule and photocatalyst [22,29,30].

XPS Analysis

Decoration of TiO_2 nanoparticle surface with noble-metal nanoparticles was also confirmed with the X-ray photoelectron spectroscopy (XPS) measurements (Physical Electronics 5800 spectrometer) besides oxidation states. The survey spectra of the TiO_2-AgAuNPs is given in Figure 3(a).

The survey spectrum of the TiO_2-AgAuNPs confirms the presence of major elements, Ti, Ag, and Au in the resulting nanostructure. The high-resolution XPS spectrum of Ag and Au (Figure 3(b) and (c)) also provided to prove the metallic form of the particles. According to Figure 3(b) it can be concluded that the binding energies of the Ag 3d5/2 and Ag 3d3/2 peaks corresponding to 365.0 and 371.0 eV are the indication of the metallic form of the silver. From Figure 3(c), the spin-orbit splitting value was calculated as 4 eV from the Au 4f7/2 and Au 4f5/2 peaks centered at 81.0 and 85.0 eV which is the indication of a cubic crystal structure. The results are in good agreement with TEM and EDX analysis and confirm the decoration of the TiO_2 surface with metallic nanoparticles.

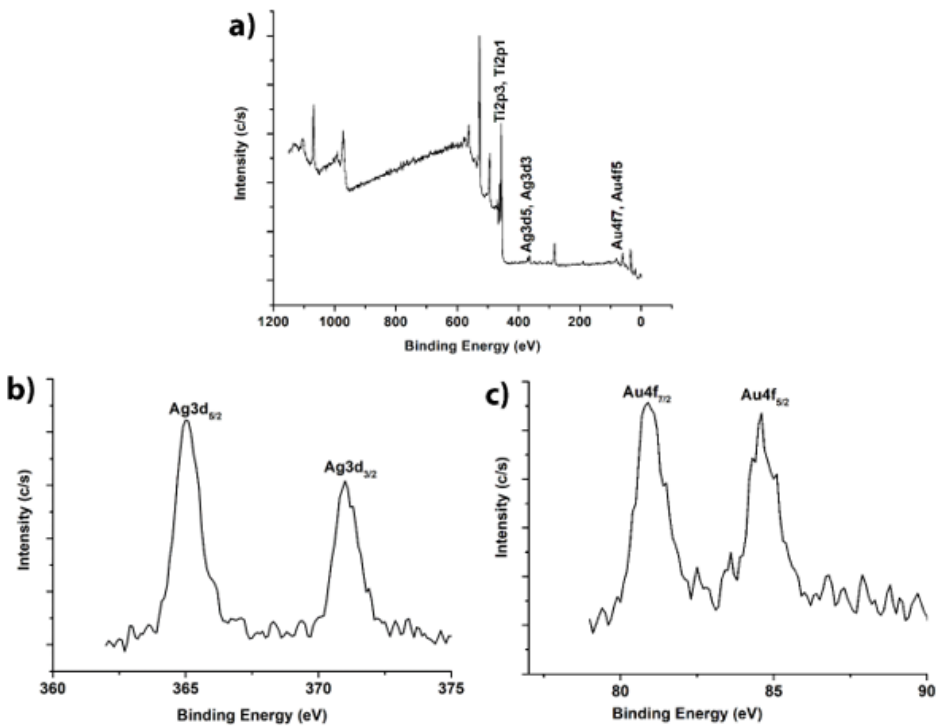

Figure 3: XPS survey (a) and high-resolution spectra of prepared TiO_2-AgAuNPs photocatalysts for Ag 3d (b), and 4f (c).

Diffuse Reflectance Spectroscopy

The optical properties of the mono bimetallic nanoparticles added TiO_2 nanoparticles were measured by UV–vis spectrometer equipped with diffuse reflectance unit (DRS) (Figure 4). The edge of the bare TiO_2 nanoparticles was located around 390 nm. The related part of the UV-Vis spectra of bare TiO_2 nanoparticles was shifted to the visible part of the spectrum after the addition of noble-metal nanoparticles to the surface which can be considered as an indication of the improvement of the visible light absorption. The band gaps of the TiO_2 and TiO_2-AgAuNPs were calculated as 3.16 eV and 2.94 eV from the absorption maxima of 392 nm and 421 nm respectively. According to the results, it can be concluded that the decoration of TiO_2 with noble metals resulted in the red-shift of the absorption band from UV to the visible part of the electromagnetic spectrum. So, ultrafine bimetallic nanoparticle added TiO_2 (TiO_2-AgAuNPs) can be a good candidate as a catalyst in the visible-light-driven photocatalytic reactions.

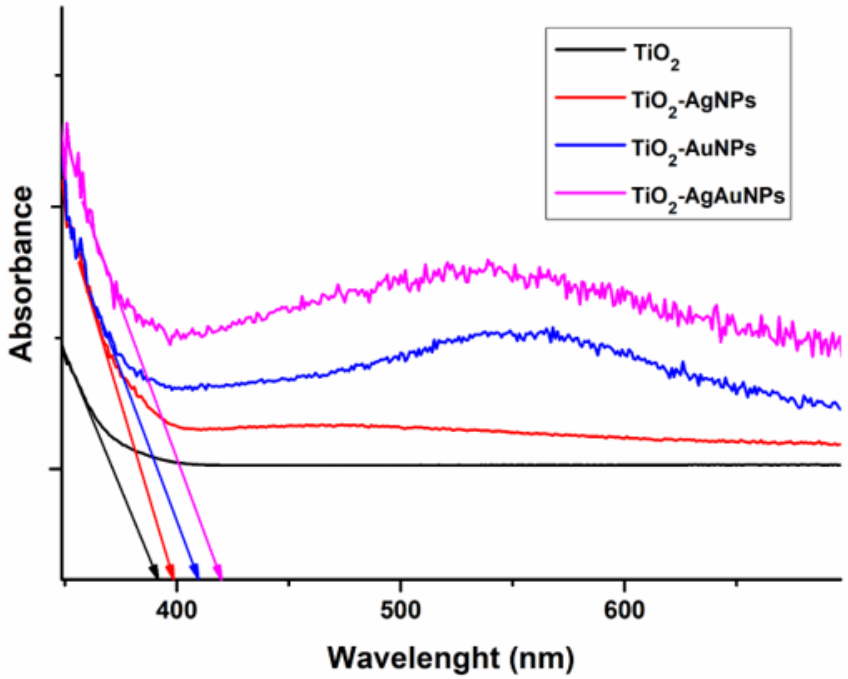

Figure 4: Diffuse reflectance UV-Vis spectra of TiO_2 nanoparticles, TiO_2-AgNPs, TiO_2-AuNPs, and TiO_2-AgAuNPs, respectively.

Photocatalytic Activity and Stability Measurements

The activity of TiO_2-AgAuNPs photocatalyst was tested in the degradation of 2×10^{-5} M MB under both UV and solar light exposure. Besides, activities of bare TiO_2 nanoparticles and Au and Ag metal added TiO_2nanoparticles produced with the same procedure were determined under the same conditions for comparison. Control experiments (a: MB and light exposure without catalyst, b: MB and catalyst without light exposure) also performed to show no change in the MB concentration. Only a slight decrease was observed in the absorption maxima of MB when treated with catalyst without light exposure due to the adsorption behavior of dye molecules. When the light was sent to the mixture of MB and catalyst, the absorption intensity of MB measured with UV-Vis spectrophotometer (Specord S 600 UV-Vis spectrophotometer) was decreased over time. The comparison of the percent degradation of dye showing the catalytic activity of the photocatalysts also given in Figure 5. The percent degradation results of MB obtained with the use of the mentioned catalysts under both UV and solar light were also summarized in Table 1.

Table 1: The percent degradation results of MB obtained with the use of the mentioned catalysts under both UV and solar light.

Photocatalyst	Light source	Exposure Time	% Degradation
TiO_2	UV	40	99.2
TiO_2-AgNPs	UV	30	99.7
TiO_2-AuNPs	UV	40	98.1
TiO_2-AgAuNPs	UV	40	97.3
TiO_2	Solar	120	96.2
TiO_2-AgNPs	Solar	120	95.6
TiO_2-AuNPs	Solar	60	99.5
TiO_2-AgAuNPs	Solar	50	99

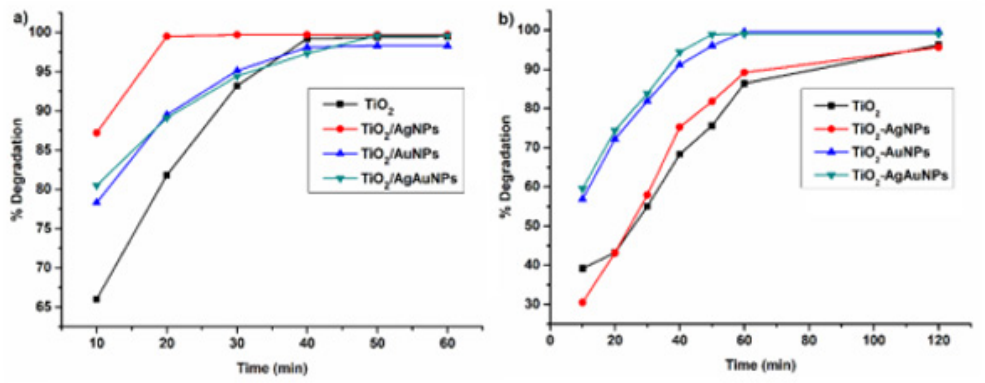

Figure 5: Comparison of the catalytic activity of the catalyst used for MB degradation under both UV (a) and solar light (b) exposure.

It can be clearly seen from the results, bimetallic silver and gold nanoparticle added TiO_2 nanoparticles, TiO_2-AgAuNPs, showed better photocatalytic activity although contains less amount of silver and gold (% 0.68 (w/w, Ag) and % 0.45 (w/w, Au)) and 99% degradation was obtained only in 50 min under solar light exposure when compared with bare TiO_2, TiO_2-AgNPs, and TiO_2-AuNPs due to greater shift of Fermi level of ultrasmall bimetallic AgAuNPs to more negative potential value which leads the enhanced interfacial charge transfer by increasing the hole numbers due to decrease in electron density in the conduction band of TiO_2. This increase produces more oxidative radicals providing the degradation of dye molecules [15,18,21,22,31-33]. This behavior also supported by the photoluminescence study. The photocatalytic degradation of organic pollutants mainly related to the number of oxidative species produced through the photocatalytic process. For this reason, in order to estimate the number of radicals generated photocatalytically, photoluminescence (PL) measurements were performed by using coumarin as a probe molecule. The hydroxyl radical produced by photocatalyst during the irradiation reacts with coumarin to form 7-hydroxycoumarin which has fluorescence intensity located at 456 nm. The effect of the photocatalyst prepared with the addition of noble metals onto the TiO_2 nanoparticles on the formation of oxidative species after 60 min of solar light exposure is shown in Figure 6(a). The lowest rate of formation of hydroxyl radicals was observed in the usage of for bare TiO_2 nanoparticles and it was increased with the addition of noble metal nanoparticles to TiO_2 nanoparticles under solar light exposure. The highest conversion of coumarin to 7-hydroxycoumarin was obtained with the usage of TiO_2-AgAuNPs as photocatalyst.

According to the results given above, it can be concluded that the addition of ultrasmall AgAuNPs with narrow size distribution on the TiO_2 nanoparticles improves the absorption property under solar light which results in enhanced photo-conversion efficiency by decreasing the probability of charge recombination between electrons and holes [15,21,22].

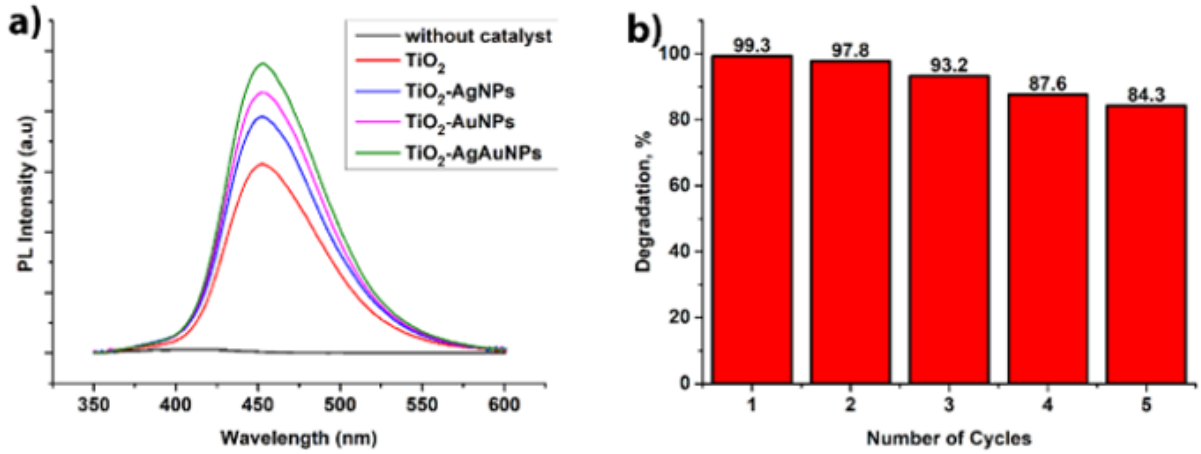

Figure 6: PL spectra of coumarin obtained with catalysts used in this study under solar light exposure ([Catalysts] = 0.5 g L^{-1}; [Coumarin] = 5 × 10^{-4} M) (a) and the reuse capacity of TiO_2-AgAuNPs as photocatalyst (b).

The recycling stability of TiO_2-AgAuNPs was investigated by performing five successive dye removal experiments under solar radiation by using the same catalyst under similar experimental conditions. Only 16% decrease was observed after five successive tries (Figure 6 (b). After 5 runs, solutions were analyzed by ICP-OES and no leaching of Au and Ag into the solution was observed. Therefore, the decrease in the catalytic activity of TiO_2-AgAuNPs, after the 5th run in photocatalytic degradation of MB can be attributed to partial oxidation of noble metal nanoparticles and deposition of degradation products onto the catalyst besides a small amount of loss of catalyst during separation.

The photocatalytic degradation process can be followed in two different ways. In the first one, the decolorization of dye followed by using a UV-Vis spectrometer. But it is difficult to understand whether the removal is caused by photocatalytic degradation or attachment to the surface of the material (adsorption). In order to decide whether the process is degradation or not, the removal of the MB dye was due to photocatalytic degradation was revealed by LC-MS data. TiO_2 nanoparticles are considered as the reference total oxidation catalyst in photocatalytic reactions. Thus the data obtained from the usage of TiO_2 nanoparticle for the decomposition of methylene blue was used to prove the photocatalytic decomposition of methylene blue with the usage of prepared composite material under solar light illumination. The corresponding MS data of the methylene blue before and after the photocatalytic reaction is given in Figure 7.

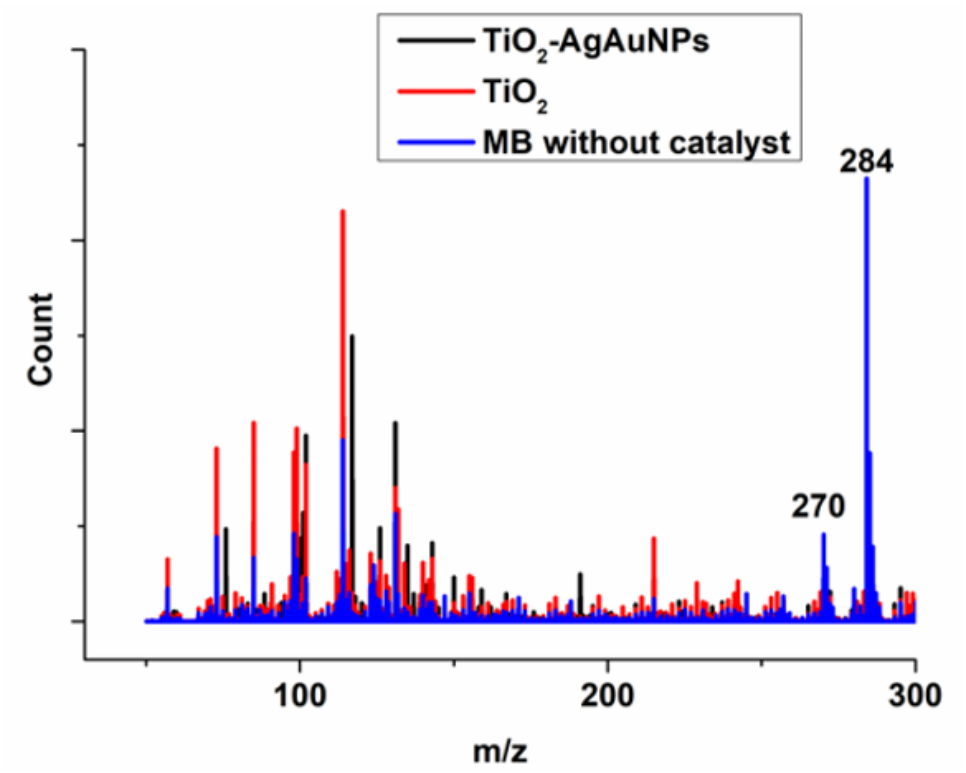

Figure 7: LC-MS spectrum of MB before the photocatalytic reaction and after treatment with TiO_2 nanoparticles and TiO_2-AgAuNPs under solar light.

The line located at m/z=284 is related to the parent ion of methylene blue $[MB + H]^+$. The other intense line observed at m/z= 270 is related to Azure B known as well-known homologs of MB [34]. New lines at m/z= 131, 114, 98, 85 and 73 are related to fragmentation of MB and/or organic contamination. The main signals located at m/z= 284 and m/z= 270 were disappeared after the photocatalytic treatment with TiO_2 and TiO_2-AuAgNPs catalysts under solar light irradiation, respectively which is the indication of degradation of MB molecules. The results of LC-MS measurements are consistent with the results obtained with UV-Vis spectrometry in decolorization studies. As can be seen from the MS spectra, there is a decrease in the total amount of methylene blue (Figure 7) which can be attributed to the decomposition of it into CO_2 and other inorganic ions like nitrate and sulfate besides degradation products and fragments. When the total illumination time of solar light considered (120 min for TiO_2 nanoparticles and 50 min for TiO_2-AuAgNPs), it is possible to say that the TiO_2-AuAgNPs is a much more effective catalyst than TiO_2 nanoparticles in the degradation of dye molecules.

Hydrogen Generation Capacity Measurements

Besides the dye removal studies, the photocatalytic perfor-

mance of the TiO_2-AgAuNPs catalyst was investigated in hydrogen generation from water/ethanol mixture under UV light exposure. Total gas formation during the reaction was followed and obtained results are given in Figure 8. As seen from Figure 8, the minimum gas evolution was observed in the use of bare TiO_2 nanoparticles. When the noble metals added to TiO_2 nanoparticles, the amount of gas evolved was increased and the highest amount of evolution was obtained with the usage of TiO_2-AgNPs and TiO_2-AgAuNPs as photocatalyst under UV light irradiation. The amount of hydrogen in the formed gas was found with GC measurements coupled with a TCD detector. Calculated amounts of hydrogen for each catalyst are given in Table 1.

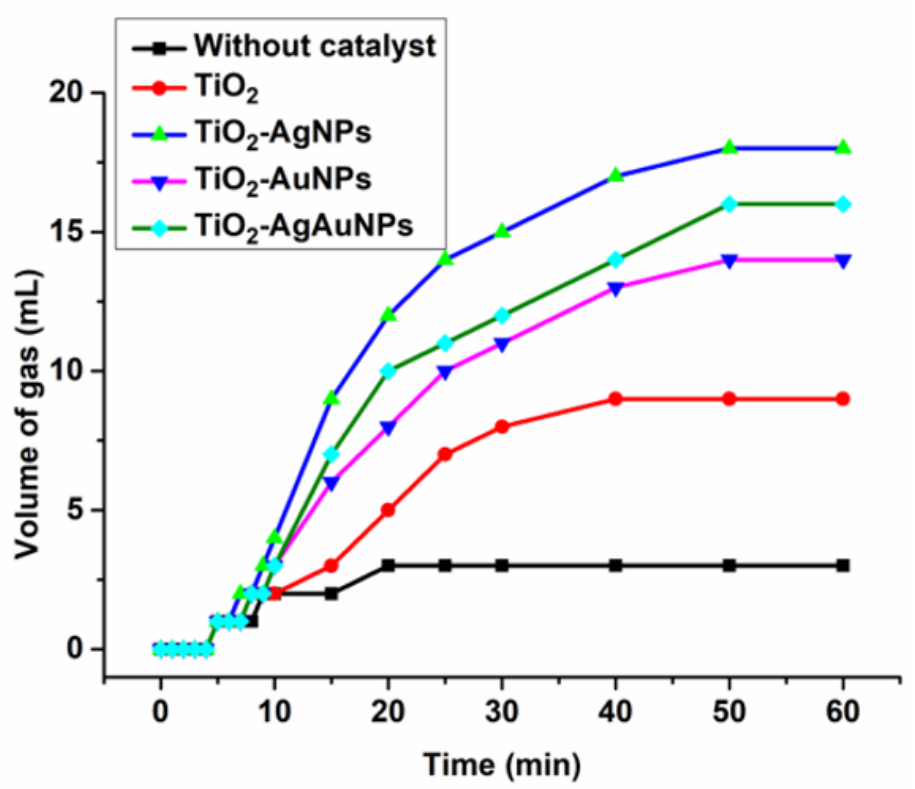

Figure 8: The comparison of the volume of the evolved gas obtained from the water-ethanol mixture with the use of TiO_2 nanoparticles, TiO_2-AgNPs, TiO_2-AuNPs, and TiO_2-AgAuNPs under UV light exposure.

Table 2: Amount of hydrogen produced from the ethanol-water mixture under UV light exposure (Temperature of the reactor was measured around 305 K at the end of the reaction)

Sample	The volume of gas (mL)	% Hydrogen in gas	Amount of hydrogen (mol)
Without catalyst	3	0	0
TiO_2	9	1.60%	5.75×10^{-6}
TiO_2-AgNPs	18	3.50%	2.52×10^{-5}
TiO_2-AuNPs	14	3.20%	1.79×10^{-5}
TiO_2-AgAuNPs	16	3.40%	2.17×10^{-5}

The improved activity of metal loaded TiO_2 catalysts can be related to the interaction of TiO_2 and ultrasmall sized metallic and bimetallic noble metal nanoparticles which provide better charge separation and low electron-hole recombination. The higher catalytic activity of TiO_2-AgNPs in hydrogen generation under UV light can be attributed to surface plasmons located around 410 nm, which is closer to the UV region when compared with gold and silver-gold bimetallic nanoparticles.

Conclusion

Commercially available TiO_2 nanoparticles were decorated with ultra-small bimetallic AuAgNPs by using a simple, fast and green method. Red-shift in the bandgap of bare TiO_2 nanoparticles was observed with the addition of bimetallic AgAuNPs nanoparticles and the resulting structure, TiO_2-AgAuNPs, showed higher catalytic activity and good stability and reproducibility, compared with bare TiO_2, TiO_2-AgNPs, and TiO_2-AuNPs in dye removal and hydrogen generation reactions. The improved photocatalytic activity can be attributed to the ultrasmall size and well-distributed AgAuNPs decorated on TiO_2 nanoparticles which led the efficient photo-induced electron-hole pairs separation and interfacial charge transfers. The PL study which shows the number of oxidative species produced with catalysts also supports the photocatalytic activity of TiO_2-AgAuNPs catalysts. Total removal of MB dye within 40 minutes was observed under solar light with the usage of TiO_2-AgAuNPs as photocatalyst. Thus TiO_2-AgAuNPs can be a good candidate for the removal of dye molecules founded in the textile-based wastewater under sunlight and photocatalytic hydrogen production from volatile organic compounds founded in wastewater.

Acknowledgment

The authors would like to thank TÜBİTAK for financial support (Grant no: 115Z151) and METU Central Laboratory for characterizations.

Conflict of Interest

None.

References

1. R P Schwarzenbach, B I Escher, K Fenner, T B Hofstetter, C A Johnson, et al. (2006) Science 313: 1072-1077.
2. I K Konstantinou, T A Albanis (2004) Appl Catal. B: Environ 49: 1-14.
3. A Patsoura, D I Kondarides, X E Verykios (2007) Catal. Today 124: 94-102.
4. J Yuan, X Liu, Y Tang, Y Zeng, L Wang, et al. (2018) Appl Catal B: Environ 237: 24-31.
5. P Zhu, Y Chen, M Duan, Z Ren, M Hu, et al. (2018) Catal. Sci. Technol 8: 3818-3832.
6. R K Chava, J Y Do, M Kang, (2019) J Mater Chem A 7: 13614-13628.
7. N L Panwar, S C Kaushik, S Kothari (2011) Renew Sustain. Energy Rev 15: 1513-1524.
8. P A Owusu, S A Sarkodie (2016) Cogent Eng 3: 1-14.
9. A Sumboja, T An, H Y Goh, M Lübke, D P Howard, et al. (2018) ACS Appl Mater. Interfaces 10: 15673-15680.
10. A Fujishima, K Honda (1972) Nature 238: 37-38.
11. M Pelaez, N T Nolan, S C Pillai, M K Seery, P Falaras, et al. (2012) Appl Catal. B: Environ 125: 331-349.
12. Z Hai, N E Kolli, D B Uribe, P Beaunier, M J Yacaman, et al. (2013) J Mater. Chem A 1: 10829-10835.
13. S M Gupta, M Tripathi (2011) Chinese Sci. Bulletin 56: 1639-1657.
14. S Linic, P Christopher, D B Ingram (2011) Nat Mater 10: 911-921.
15. V Subramanian, E E Wolf, P V Kamat (2004) J Am Chem. Soc 126: 4943-4950.
16. R Kaur, B Pal, J Mol (2012) Catal. A: Chem 355: 39-43.
17. M Murdoch, G I N Waterhouse, M A Nadeem, J B Metson, M A Keane, et al. (2011) Nat Chem. 3: 489-492.
18. C Chen, W Ma, J Zhao (2010) Chem Soc. Rev 39: 4206-4219.
19. S G Kumar, L G Devi (2011) J Phys. Chem A 115: 13211-13241.
20. A Primo, A Corma, H García (2011) Phys Chem. Chem Phys 13: 886-910.
21. A Tanaka, S Sakaguchi, K Hashimoto, H Kominami (2013) ACS Catal 3: 79-85.
22. D Tsukamoto, Y Shiraishi, Y Sugano, S Ichikawa, S Tanaka, et al. (2012) J Am Chem. Soc 134: 6309-6315.
23. S C Chan, M A Barteau (2005) Langmuir 21: 5588-5595.
24. E Kowalska, O O P Mahaney, R Abe, B Ohtani (2010) Phys Chem. Chem Phys12: 2344-2355.
25. C G Silva, R Juarez, T Marino, R Molinari, H Garcia (2011) J Am. Chem Soc 133: 595-602.
26. D Wang, Z H Zhou, H Yang, K B Shen, Y Huang, et al. (2012) J Mater. Chem 22: 16306-16311.
27. K S Suslick, T Hyeon, M Fang (1996) Chem. Mater 8: 2172-2179.
28. P A Kolinko, D V Kozlov (2009) Appl Catal. B: Environ 90: 126-131.
29. N Pugazhenthiran, S Murugesan, S Anandan, J Hazard (2013) Mater 263: 541-549.
30. A ZJurek, E Kowalska, J W Sobczak, W Lisowski, B Ohtani, (2011) Appl Catal. B: Environ 101: 504-514.
31. S Anandan, M Ashokkumar (2009) Ultrason. Sonochem. 16: 316-320.
32. M Murdoch, G I N Waterhouse, M A Nadeem, J B Metson, M A Keane, et al. (2011) Nat. Chem 3: 489-492.
33. S A A Vandarkuzhali, N Pugazhenthiran, R V Mangalaraja, P Sathishkumar, B Viswanathan, et al. (2018) ACS Omega 3: 9834-9845.
34. M A Rauf, M A Meetani, A Khaleel, A Ahmed (2010) Chem. Eng J 157: 373-378.